Published OnlineFirst March 8, 2013; DOI: 10.1158/1535-7163.MCT-12-0949

Molecular Cancer Therapeutics

Bcl-2/Bcl-x_L Inhibition Increases the Efficacy of MEK Inhibition Alone and in Combination with PI3 Kinase Inhibition in Lung and Pancreatic Tumor Models

Nguyen Tan[1], Maureen Wong[1], Michelle A. Nannini[1], Rebecca Hong[1], Leslie B. Lee[1], Stephen Price[2], Karen Williams[2], Pierre Pascal Savy[2], Peng Yue[1], Deepak Sampath[1], Jeffrey Settleman[1], Wayne J. Fairbrother[1], and Lisa D. Belmont[1]

Abstract

Although mitogen-activated protein (MAP)–extracellular signal-regulated kinase (ERK) kinase (MEK) inhibition is predicted to cause cell death by stabilization of the proapoptotic BH3-only protein BIM, the induction of apoptosis is often modest. To determine if addition of a Bcl-2 family inhibitor could increase the efficacy of a MEK inhibitor, we evaluated a panel of 53 non–small cell lung cancer and pancreatic cancer cell lines with the combination of navitoclax (ABT-263), a Bcl-2/Bcl-x_L (BCL2/BCL2L1) antagonist, and a novel MAP kinase (MEK) inhibitor, G-963. The combination is synergistic in the majority of lines, with an enrichment of cell lines harboring KRAS mutations in the high synergy group. Cells exposed to G-963 arrest in G_1 and a small fraction undergo apoptosis. The addition of navitoclax to G-963 does not alter the kinetics of cell-cycle arrest, but greatly increases the percentage of cells that undergo apoptosis. The G-963/navitoclax combination was more effective than either single agent in the KRAS mutant H2122 xenograft model; BIM stabilization and PARP cleavage were observed in tumors, consistent with the mechanism of action observed in cell culture. Addition of the phosphatidylinositol 3-kinase (PI3K, PIK3CA) inhibitor GDC-0941 to this treatment combination increases cell killing compared with double- or single-agent treatment. Taken together, these data suggest the efficacy of agents that target the MAPK and PI3K pathways can be improved by combination with a Bcl-2 family inhibitor. *Mol Cancer Ther; 12(6); 853–64. ©2013 AACR.*

Introduction

Recent advances in cancer drug therapies associated with targeting oncogenic "drivers" have shown tremendous potential for improving clinical benefit. However, a major limitation to the overall benefit from targeted therapy is the development of drug resistance. Resistance can occur because of mutations that render the drug target insensitive to the inhibitor or when cancer cells change their dependency on the pathway that is targeted. In the first example, resistance can be overcome by developing new drugs that effectively inhibit resistance-associated mutants, as in the example of dasatinib and nilotinib, which are effective on BCR/ABL mutants that confer resistance to imatinib (1). Another approach is to target multiple signaling pathways simultaneously, and thus prevent the cancer cell from changing its dependency to another signaling pathway. There is considerable preclinical evidence supporting this approach, for example, in the setting of combining inhibitors of mitogen-activated protein (MAP)–extracellular signal-regulated kinase (ERK) kinase (MEK; MAP kinase kinase, MAP2K) with inhibitors of PI3 kinase (phosphatidylinositol 3-kinase, PIK3CA) or (2–7) BRAF (8–10), and these combinations are beginning to show efficacy in the clinic (11). A third approach to enhancing the efficacy of targeted therapy is to simultaneously target downstream proteins that protect tumor cells from apoptosis and thus increase overall cell killing (12–14). This strategy relies on increasing cancer cell cytotoxicity cells to decrease the probability that a cell will survive to develop resistance. In addition, altering upstream dependencies will be of no avail because the signaling pathways ultimately converge on these downstream apoptotic pathways. Here, we have explored the combination of an MEK kinase inhibitor and a Bcl-2/Bcl-x_L inhibitor to evaluate the potential utility of this combination treatment strategy.

MEK transduces signals downstream of the EGFR, RAS, and RAF proteins, and activating mutations in any of these proteins can lead to enhanced MEK activity. MEK activation in turn produces prosurvival signals via inhibition of the proapoptotic BH3-only proteins BIM and

Authors' Affiliations: [1]Genentech, Inc., South San Francisco, California; and [2]Argenta Discovery Ltd., Harlow, Essex, United Kingdom

Note: Supplementary data for this article are available at Molecular Cancer Therapeutics Online (http://mct.aacrjournals.org/).

Corresponding Author: Lisa D. Belmont, Genentech, Inc., 1 DNA Way, South San Francisco, CA 94080. Phone: 650-467-7462, Fax: 650-742-5179; E-mail: belmont.lisa@gene.com

doi: 10.1158/1535-7163.MCT-12-0949

Published OnlineFirst March 8, 2013; DOI: 10.1158/1535-7163.MCT-12-0949

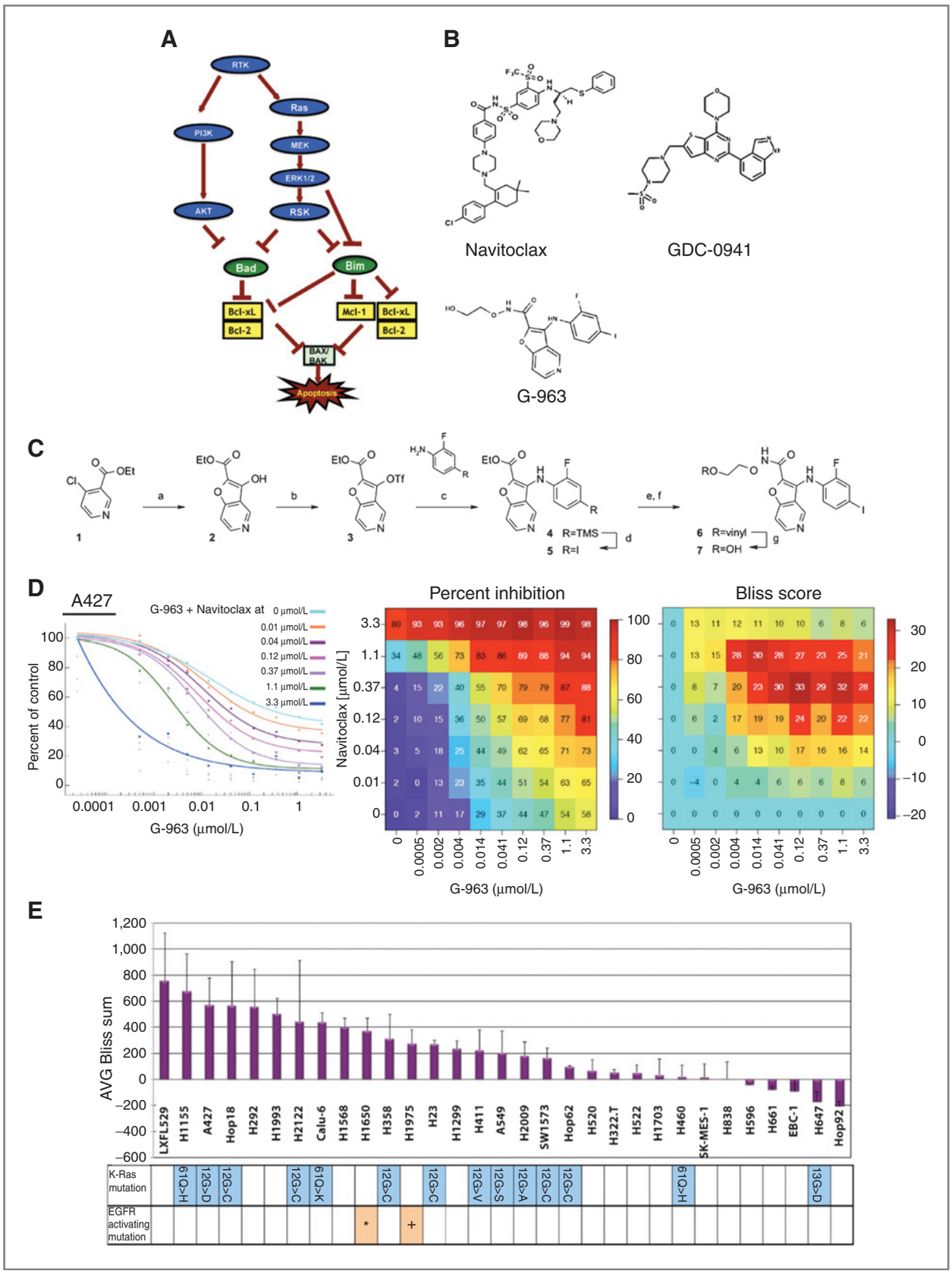

Published OnlineFirst March 8, 2013; DOI: 10.1158/1535-7163.MCT-12-0949

BAD and stabilization of the antiapoptotic Bcl-2 family member, MCL1. MEK activates ERK1/2 (MAPK1, MAP3K2), which subsequently phosphorylates BIM on Ser69, priming it for phosphorylation by p90RSK, and ultimately resulting in its ubiquitination and proteasomal degradation (15). In addition, ERK1/2-mediated phosphorylation of FOXO3A promotes its degradation and thus inhibits FOXO3A-dependent transcription of BIM (16). ERK1/2 also directly activates p90RSK, which inactivates BAD. RSK phosphorylates BAD on Ser112 facilitating its binding to 14-3-3, which acts to sequester and inhibit its proapoptotic activity. Activation of ERK1/2 is reported to stabilize the antiapoptotic protein, MCL1 (17). Thus, the inhibition of MEK is expected to promote apoptosis by increasing BIM levels (both by transcriptional activation and protein stabilization), by activating BAD via reducing inhibitory phosphorylation, and by decreasing levels of MCL1 through promotion of its proteasomal degradation (Fig. 1A).

Bcl-2 family members sequester and inhibit the "executioner" proteins BAX and BAK (BAK1), which form pores in the mitochondrial outer membrane and allow cytochrome C release (18). The antiapoptotic Bcl-2 family members include Bcl-2, Bcl-x_L, MCL1, BCL2A1, and Bcl-w (BCL2L2). Of these, Bcl-2, Bcl-x_L, and MCL1are expressed in solid tumors. Inhibition of MEK neutralizes Bcl-2 and Bcl-x_L by increasing the levels of functional BIM and BAD, and it neutralizes MCL1 by destabilizing MCL1 protein and by stabilizing its antagonist, BIM. However, the activation of BAD is vulnerable step in this mechanism because compensatory activation of the PI3K pathway can inhibit BAD via phosphorylation on Ser136. Addition of navitoclax, a "BAD mimetic" that is not subject to the phosphorylation events that inactivate BAD (19) could potentially overcome mechanisms of resistance that rely on inhibition of BAD. Furthermore, the MEK inhibitor/navitoclax combination may increase efficacy in cases where MEK inhibition alone results in less than complete blockade of Bcl-x_L and Bcl-2 activities.

Navitoclax has been shown to enhance the activity of chemotherapeutic agents (20–24). However, studies on its ability to enhance targeted therapy have been limited. Cragg and colleagues showed BIM-dependent combination efficacy of a MEK inhibitor and ABT-737, a compound with similar biochemical activity to navitoclax, in several BRAF mutant models (12). Konopleva and colleagues showed similar combination efficacy in AML models (25). In this work, we set out to determine the effectiveness of a navitoclax/MEK inhibitor combination in a large panel of non–small cell lung cancer (NSCLC) and pancreatic ductal adenocarcinoma derived cell lines with the aim of (1) determining the prevalence of MEK inhibitor/navitoclax synergy in cancer lines that frequently harbor activating KRAS mutations, (2) identifying predictive biomarkers for the combination in these cancers, and (3) evaluating combination mechanism of action. In addition, we evaluated the combination mechanism of a triple combination of navitoclax with a MEK inhibitor and a PI3K inhibitor.

Materials and Methods

Chemicals

Z-VAD-FMK (Promega), necrostatin-1 (Tocris Bioscience), Navitoclax (Abbott Laboratories), G-963, and GDC-0941 (Genentech, Inc.) were dissolved in dimethyl sulfoxide (DMSO; Sigma-Aldrich).

Cell culture, antibodies, and reagents

Cell lines were obtained from the American Type Culture Collection or Deutsche Sammlung von Mikroorganismen und Zellkulturen (DSMZ), expanded, and stored at early passage in a central cell bank. Lines were authenticated by short tandem repeat (STR) and genotyped upon reexpansions. Cells were grown in RPMI 1640 medium supplemented with 10% FBS and 2 mmol/L glutamine (Invitrogen) and passaged no more than 20 times after thawing. Antibodies directed against the following proteins were used: phospho-ERK, ERK1/2, phospho-RSK, RSK1, phospho-BAD, BIM, phospho-BIM, Bcl-x_L, MCL1, p21, p27, PARP, phospho-S6 (Cell Signaling Technology), BAD (Santa Cruz Biotechnology), γ-H2AX (Millipore), MCL1 (BD Biosciences), BIM (Enzo Life Sciences), β-actin (Sigma-Aldrich), and HRP-conjugated horse anti-mouse and goat anti-rabbit antibodies (Vector Laboratories).

Biochemical assays, Western blotting, and immunoassays

Activity on purified MEK1 was measured with a homogenous time resolved fluorescence (HTRF) assay. Selectivity was measured at 1 μmol/L using a Z′-Lyte Kinase Assay Kit using Invitrogen's SelectScreen Kinase Profiling Service. To examine protein expression, cells were lysed in ice-cold RIPA buffer (Cell Signaling Technology) containing 1 mmol/L Peflabloc, Phosphatase Inhibitor Cocktail 1 and 2 (Sigma-Aldrich), and complete EDTA-free protease inhibitor tablet (Roche). Equal amounts of protein were subjected to SDS-PAGE (4–12% Bis-Tris; Invitrogen), and protein levels were evaluated by Western blotting. Solid-phase microspot

Figure 1. Navitoclax enhances the activity of G-963 in NSCLC cell lines. A, MAPK and PI3K pathway regulation of intrinsic apoptosis. B, chemical structures of navitoclax (ABT-263), G-963, and GDC-0941. C, general synthetic strategy for G-963: ethyl glycolate, NaH, DMF, 0°C to rt, 16 hours (86%; a); TfNPh2, DIPEA, DME, 95°C, 35 minutes (80%; b); Pd2(dba)3, XantPhos, K3PO4, 105°C, 24 hours (93%; c); AgBF4, ICl, DCM, −50°C, 1 hour (86%; d); 1 mol/L NaOH, EtOH, 65°C, 1.5 hours (e); H2C = CH-O(CH2)2ONH2, HOBT, EDCI, DIPEA, THF, rt, 18 hours (60% over 2 steps; f); 1 mol/L HCl, MeOH, EtOH, rt, 1.5 hours (91%; g). D, example of synergistic activity of navitoclax and G-963 in A427 cells. Left, G-963 dose–response curves in the presence of various doses of navitoclax; middle, heat map of growth inhibition; and right, heat map of Bliss scores. E, average Bliss sums and mutational status of EGFR and KRAS across the NSCLC panel. For EGFR mutation status, *, DEL.745KELREA > K; +, 790T > M, 858L > R. Error bars, SD.

Published OnlineFirst March 8, 2013; DOI: 10.1158/1535-7163.MCT-12-0949

immunoassays from Meso Scale Discovery (MSD) were also used to determine protein expression.

Combination matrices

Cells were seeded in 384-well plates at 3,000 cells/well. After 24 hours, cells were treated with navitoclax (dose range of 14 nmol/L–3.3 μmol/L) and G-963 (dose range of 1.5 nmol/L–3.3 μmol/L) in a 7 × 9 matrix. Each treatment was done in quadruplicate wells. Cells were treated for 72 hours, and ATP was determined with CellTiter-Glo (Promega). The experiment was done at least thrice, and the data are presented as an average of all runs. G-963 IC_{50} values were calculated from the 9 single-agent doses using a 4 parameter fit with XLFit (IDBS). The Bliss expectation was calculated with the equation $(A + B) - A \times B$, where A and B are the fractional growth inhibitions induced by agents A and B at a given dose. The difference between Bliss expectation and observed growth inhibition induced by the combination of agents A and B is the "Bliss excess" (26). For triple combinations, the experiment was done exactly as that of the double combination study, with or without the addition of GDC-0941 (1 μmol/L) to all wells. Two independent runs of the triple combinations were done on each cell line.

Caspase assay

Cells were seeded in 96-well plates at 5,000 cells/well. After 24 hours, cells were treated as indicated and caspase activity was determined (Promega Caspase-Glo 3/7). Data are presented as an average of 2 runs each done in duplicate.

Flow cytometry

Adherent cells were detached with EDTA (10 mmol/L), collected by centrifugation for 5 minutes at 300 × *g*, washed with PBS, fixed in ice cold 90% methanol. Cells were collected by centrifugation, washed, stained with 10 μg/mL propidium iodide (Sigma-Aldrich) and analyzed by flow cytometry (10,000 cells per treatment).

In vivo studies

Human NSCLC H2122 cells were implanted subcutaneously in the hind flank of female NCR nude mice (Taconic Farms). Tumors were monitored until they reached a mean tumor volume of 250-350 mm^3 and distributed into groups of 8 animals before initiating dosing. Navitoclax was dissolved in 60% Phosal 50 PG, 30% PEG 400, 10% EtOH vehicle, and dosed daily by oral administration. G-963 was diluted in 0.5% methycellulose/0.2% Tween-80 (MCT) and dosed daily by oral administration. Tumor volume was measured in 2 dimensions (length and width), using Ultra Cal IV calipers (Model 54 10 111; Fred V. Fowler Company), as follows: tumor volume (mm^3) = (length × $width^2$) × 0.5 and analyzed using Excel version 11.2 (Microsoft Corporation). Animal body weights were measured using an Adventurer Pro AV812 scale (Ohaus Corporation). Percent weight change was calculated as follows: body weight change (%) = $[(weight_{day\ new} - weight_{day\ 0})/weight_{day\ 0}] \times 100$. Tumor sizes and mouse body weights were recorded twice weekly over the course of treatment, and the mice were observed daily. A linear mixed modeling approach was used to analyze the repeated measurement of tumor volumes and body weight from the same animals over time (27). This approach addresses both repeated measurements and modest dropouts because of any nontreatment-related death of animals before study end. Cubic regression splines were used to fit a nonlinear profile to the time courses of log2 tumor volume at each dose level. These nonlinear profiles were related to dose within the mixed model. Tumor growth inhibition as a percentage of vehicle control (% TGI) was calculated as the percentage of the area under the fitted curve (AUC) for the respective dose group per day in relation to the vehicle, using the following formula: $\%\ TGI = 100 \times (1 - AUC_{dose}/AUC_{veh})$. Data were analyzed using R, version 2.8.1 (R Development Core Team 2008; R Foundation for Statistical Computing), the mixed models were fitted within R using the nlme package, version 3.1-89, and plotted using Prism 5 software (GraphPad Software, Inc.). For pharmacodynamic studies, tumor samples were immediately frozen in liquid nitrogen. Tumors were dissociated in cell extraction buffer and lysates analyzed by Western blotting.

Image processing and statistics

Relative protein levels were quantified using the ImageJ software (National Institutes of Health), and normalized to β-actin. Statistical analysis was done using Prism 5 (GraphPad Software) to determine the ρ (rho) value (Spearman ranking) and *P* value (2-tailed).

Results

Navitoclax enhances the activity of a MEK inhibitor in cancer cell lines

We selected navitoclax, a dual Bcl-2/Bcl-x_L inhibitor that is the subject of clinical trials (28–31), and a novel MEK inhibitor, G-963 (Fig. 1B), to test the combination efficacy associated with targeting these proteins. The general synthetic route for G-693 is shown (Fig. 1C) and a detailed route is described in the supplementary material (Supplementary Fig. S1). G-963 has an IC_{50} of 4 nmol/L (SD = 1.6) on purified MEK1, and is selective for MEK1 and MEK2 across a panel of 100 kinases (Supplementary Fig. S2). G-963 was active in 39% of the lines in a panel of 31 NSCLC cell lines, with cellular IC_{50} values ranging from 3 to 600 nmol/L. The majority of responsive cell lines ($IC_{50} < 1$ μmol/L) harbored activating mutations in EGFR or KRAS (Table 1), consistent with reports that activating KRAS mutations generally correlate with greater sensitivity to single-agent MEK inhibition (32–35). To evaluate the potential benefit of combining an MEK inhibitor and a Bcl-2/Bcl-x_L inhibitor, we employed a dose matrix to sample a large range of concentrations and concentration ratios and analyzed combination effects using the Bliss independence model. Positive Bliss

Published OnlineFirst March 8, 2013; DOI: 10.1158/1535-7163.MCT-12-0949

Table 1. Summary of combination matrices for navitoclax and G-963 in NSCLC cell lines

Cell line	Avg. Bliss sum	SD of Bliss sum	Avg.% inhibition of combination (navitoclax 3.3 μmol/L and G-963 3.3 μmol/L)	SD of % inhibition of combination	% Inhibition of G-963 (3.3 μmol/L)	SD of % inhibition of G-963	% Inhibition of navitoclax (3.3 μmol/L)	SD of % inhibiton of navitoclax	G-963 IC_{50} (μmol/L)	SD of G-963 IC_{50}	Navitoclax IC_{50} (μmol/L)	SD of navitoclax IC_{50}	KRAS	EGFR	PIK3CA	PTEN
LXFL529	756	367	91.8	5.6	31.1	9.6	45.5	10.3	NA	NA	NA	NA	WT	WT	542E > K	WT
H1155	674	288	99.8	0.0	35.1	6.4	99.5	0.1	NA	NA	0.76	0.51	61Q > H	WT	WT	null
A427	572	207	99.1	0.1	57.8	2.6	88.4	7.2	0.43	0.13	1.18	0.39	12G > D	WT	WT	WT
Hop18	568	338	85.3	1.3	36.1	6.8	34.8	8.2	NA	NA	NA	NA	12G > C	WT	WT	WT
H292	559	284	93.6	7.3	62.2	16.5	47.3	24.2	0.03	0.04	NA	NA	WT	WT	WT	WT
H1993	502	119	98.9	0.6	83.0	6.0	63.7	21.3	0.09	0.07	0.83	0.90	WT	WT	WT	WT
H2122	444	467	88.7	2.0	69.6	13.6	17.7	8.6	0.54	0.61	NA	NA	12G > C	WT	WT	WT
Calu-6	438	72	94.0	2.6	88.4	3.1	37.6	9.1	0.02	0.004	NA	NA	61Q > K	WT	WT	WT
H1568	400	69	93.4	1.5	38.4	11.0	72.3	10.1	NA	NA	1.76	0.49	WT	WT	WT	WT
H1650	374	96	83.4	2.2	17.8	8.9	54.2	2.2	NA	NA	NA	NA	WT	DEL 745KELREA > K	WT	null
H358	314	187	86.8	7.0	71.5	3.1	14.6	16.7	0.12	0.10	NA	NA	12G > C	WT	WT	WT
H1975	276	102	83.2	5.1	63.3	6.6	44.8	5.6	0.21	0.11	NA	NA	WT	790T > M, 858L > R	118G > D	WT
H23	271	28	89.9	5.6	69.7	6.1	48.8	15.8	0.04	0.04	NA	NA	12G > C	WT	WT	WT
H1299	236	59	60.5	5.8	55.7	4.8	2.0	2.7	0.61	0.97	NA	NA	WT	WT	WT	WT
H441	225	156	71.1	17.9	32.6	8.0	36.0	18.8	NA	NA	NA	12G>V	WT	WT	WT	
A549	201	171	93.1	3.7	71.5	19.0	46.5	16.5	0.15	0.17	NA	NA	12G > S	WT	WT	WT
H2009	180	105	85.6	2.8	74.6	9.2	11.7	7.5	0.10	0.13	NA	NA	12G > A	WT	WT	WT
SW1573	167	73	63.8	10.9	16.3	6.4	36.5	4.5	NA	NA	NA	NA	12G > C	WT	WT	WT
Hop62	97	9	51.2	5.1	44.0	0.1	6.4	4.2	NA	NA	NA	NA	12G > C	WT	WT	WT
H520	67	84	39.2	5.1	16.9	22.2	21.3	5.2	NA	NA	NA	NA	WT	WT	WT	null
H322.T	53	24	67.9	2.1	49.2	2.0	16.8	13.4	NA	NA	NA	NA	WT	WT	WT	WT
H522	52	59	25.0	15.1	17.2	6.3	2.1	2.0	NA	NA	NA	NA	WT	WT	WT	WT
H1703	36	121	32.7	6.3	1.3	1.9	24.0	1.6	NA	NA	NA	NA	WT	WT	WT	WT
H460	20	90	35.5	4.0	32.9	3.4	0.9	1.6	NA	NA	NA	NA	61Q > H	WT	545E > K	WT
SK-MES-1	18	99	66.3	12.3	36.8	9.3	18.6	5.2	NA	NA	NA	NA	WT	WT	WT	WT
H838	2	133	37.8	6.1	32.4	4.9	8.4	0.8	NA	NA	NA	NA	WT	WT	WT	WT
H596	−44	6	63.8	4.3	30.8	9.0	36.4	2.3	NA	NA	NA	NA	WT	WT	545E > K	WT
H661	−81	24	65.8	8.1	35.4	6.3	25.7	2.7	NA	NA	NA	NA	WT	WT	WT	WT
EBC-1	−94	80	91.0	4.4	72.6	2.9	87.5	5.7	0.04	0.01	0.06	0.02	WT	WT	WT	WT
H647	−172	75	69.0	4.8	26.2	2.3	48.5	9.3	NA	NA	NA	NA	13G > D	WT	WT	WT
Hop92	−206	36	76.1	18.7	50.3	2.8	68.3	28.3	NA	NA	NA	NA	WT	WT	WT	WT

NOTE: The data reflect the average of 3 independent runs conducted in quadruplicate.

Abbreviations: NA, not applicable; WT, wild-type.

Published OnlineFirst March 8, 2013; DOI: 10.1158/1535-7163.MCT-12-0949

scores indicate combinations where the effect is greater than additive. The heat map for A427 shows that there are positive Bliss scores across a large range of concentrations for both compounds (Fig. 1D). Heat maps for cell lines that had intermediate or no synergy are in the supplementary material (Supplementary Fig. S3). To summarize these data, the Bliss scores for all dose combinations are added and referred to as the Bliss sum.

We applied this combination analysis to 31 NSCLC cell lines and 22 pancreatic cancer cell lines and found that in the majority of cell lines the treatment combination was associated with a greater than additive response (Table 1 and Supplementary Table S1). In the NSCLC panel, there was a significant enrichment for cell lines with activating mutations in EGFR or KRAS in the high synergy set ($P = 0.01$, Fishers exact test, using a cutoff Bliss Sum ≥ 100; Fig. 1E). Sensitivity to single-agent MEK inhibitor is not required for synergy, although the high synergy cell lines (Bliss sum $\geq$100) are enriched for G-963 sensitivity ($P = 0.0024$; Fishers exact test).

To identify additional biomarkers predictive of synergy, we measured baseline protein levels of BAD, pS112-BAD, BIM, MCL1, Bcl-x_L, BAX, BAK, puma by Western blot (24) and pERK and pAKT using MSD technology (data not shown), and find that the only significant correlation with Bliss sum is baseline level of pS112-BAD (Supplementary Fig. S4). We also investigated the correlation of baseline gene expression and synergy scores. However, we did not identify genes that exhibited strong correlation between expression and synergy [defined as false discovery rate (FDR) < 0.1]. For subsequent studies, we chose models harboring KRAS mutations because of the observed enrichment for KRAS mutation in high synergy lines.

MEK inhibition results in increased BIM across a panel of KRAS mutant NSCLC cell lines alone and in combination with navitoclax

To explore the mechanism underlying the observed synergy, we examined the consequences of MEK inhibition on the intrinsic apoptosis pathway across a panel of KRAS mutant NSCLC cell lines (Fig. 2A). We observed a durable suppression of ERK phosphorylation, although p90RSK phosphorylation was reduced to varying extents. BIM protein levels increased in response to MEK inhibition in all cell lines tested, irrespective of synergy scores. Most cell lines exhibit a reduction in pS112-BAD at early time points, but the kinetics of this response vary greatly between cell lines and the effect is not durable. MCL1 levels are modestly reduced in some cell lines, but frequently recover. The collective biochemical findings point to a consistent stabilization of BIM, although the effects on BAD and MCL1 are transient and vary between cell lines.

We next examined cells treated with the combination of navitoclax and the MEK inhibitor. Navitoclax did not alter ERK or p90RSK phosphorylation, and the effects of MEK inhibition on ERK and RSK phosphorylation as well as BIM stabilization are comparable following combination treatment compared with the single-agent G-963. At early time points, MCL1 levels increase in navitoclax treated cells and decrease in G-963–treated cells, and the effect is balanced out in the combination treatment setting, similar to an effect previously observed in AML models with ABT-737 and MEK inhibition (25). Overall, signaling downstream of MEK does not seem to be impacted by navitoclax, but there is enhanced PARP cleavage in all cell lines treated with the combination compared with either single-agent (Fig. 2B).

Navitoclax/G-963 combination treatment results in G_1 arrest and caspase-dependent cell death

We conducted flow cytometry of single- and double-agent–treated cells in the presence or absence of the caspase inhibitor ZVAD-FMK or the necroptosis inhibitor necrostatin and analyzed DNA content. Navitoclax alone has little effect on cells, whereas G-963 causes a G_1 arrest after 24 hours and a slight increase in the sub-2N population by 48 hours while maintaining a strong G_1 arrest (Fig. 2C and D). The combination treatment increases the sub-2N population to 25%, compared with navitoclax (3%) or G-963 (5%) alone, by 48 hours. The increase in the sub-2N population is abrogated in all drug-treated cell lines with the addition of Z-VAD-FMK, whereas the increase in the sub-2N population is still observed in the presence of necrostatin, which inhibits necroptosis by inhibition of RIP kinase (36). These data suggest that MEK inhibition leads primarily to G_1 arrest, and addition of navitoclax increases caspase-dependent cell death.

Navitoclax enhances the efficacy of G-963 in H2122 xenografts

We evaluated the effect of the combination using H2122 xenografts in nude mice. Animals bearing H2122 xenografts were dosed with G-963, navitoclax, or the combination. Single-agent navitoclax was not efficacious, whereas treatment with G-963 resulted in tumor growth delay (74% TGI). The combination of navitoclax and G-963 increased the efficacy and resulted in 99% TGI (Fig. 3A and B). The enhanced antitumor activity induced by navitoclax when combined with G-963 was statistically significant compared with single-agent G-963 treatment based on 95% confidence intervals and nonoverlapping individual tumor volumes between the 2 groups (Fig. 3B). All single-agent and combination treatments were well tolerated as indicated by minimal changes in animal body weights (data not shown). Within 4 hours of treatment, MCL1 protein levels decreased after treatment with G-963 alone or in combination with navitoclax and remained suppressed for 8 hours. Increases in BIM were observed as early as 1 hour posttreatment with G-963 and remained elevated through 8 hours. Navitoclax had no effect on MCL1or BIM protein levels nor did it alter the levels of Bcl-x_L. The combination treatment resulted in increased PARP cleavage (Fig. 3C).

Published OnlineFirst March 8, 2013; DOI: 10.1158/1535-7163.MCT-12-0949

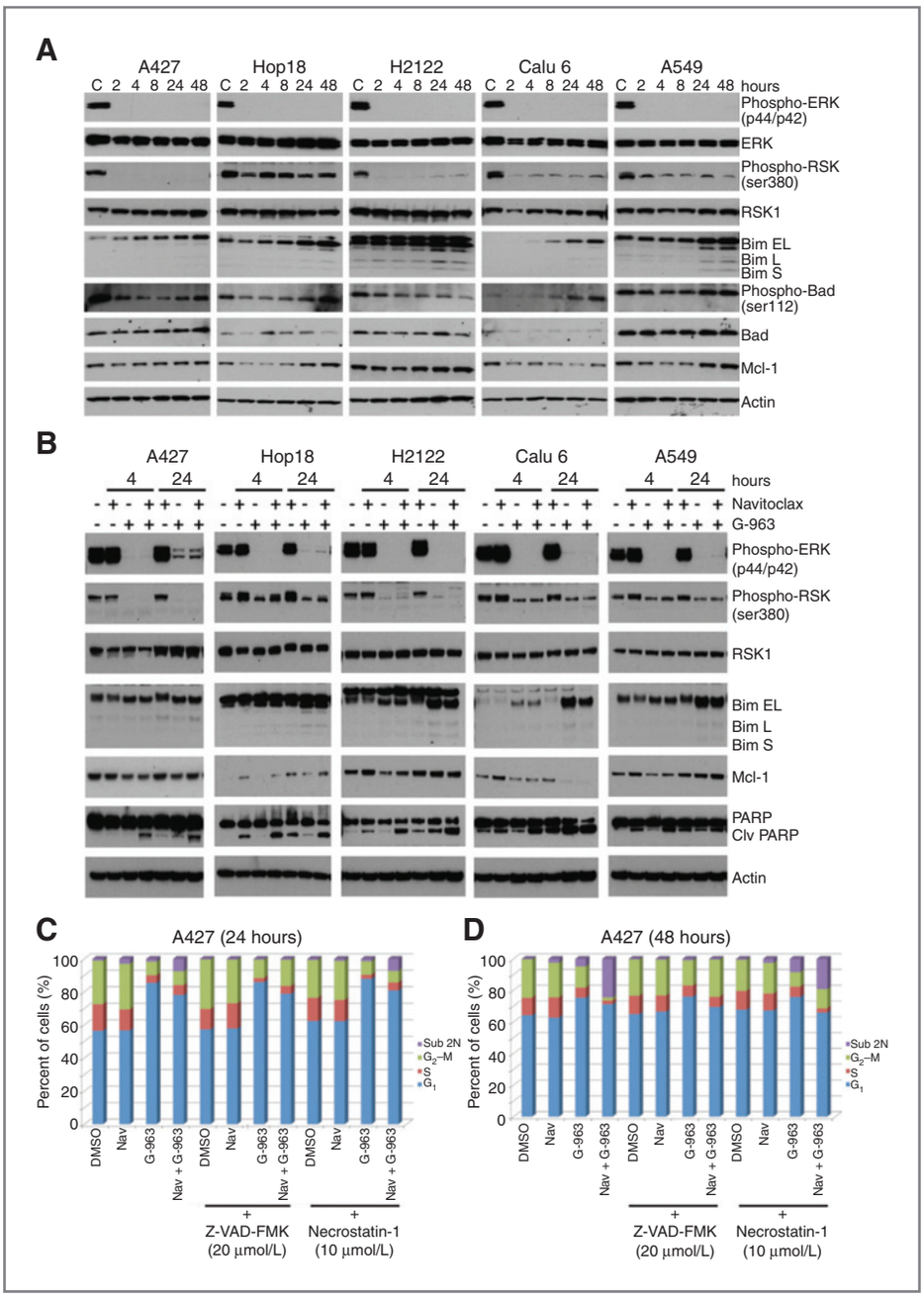

Figure 2. Cellular response to G-963 and the G-963/navitoclax combination. A, Western blots of whole cell lysates from cells treated with 2 μmol/L G-963. B, Western blots of lysates from cells treated with navitoclax (1 μmol/L), G-963 (2 μmol/L), or the combination. C, DNA content assessed by flow cytometry for A427 cells treated with navitoclax (1 μmol/L), G-963 (2 μmol/L), or the combination plus or minus Z-VAD-FMK (20 μmol/L) or necrostatin-1 (10 μmol/L) for 24 hours; D, DNA content assessed by flow cytometry for A427 cells treated with navitoclax (1 μmol/L), G-963 (2 μmol/L), or the combination plus or minus Z-VAD-FMK (20 μmol/L) or necrostatin-1 (10 μmol/L) for 48 hours.

Addition of a PI3 kinase inhibitor enhances the activity of the navitoclax/MEK inhibitor combination

Because the combination of navitoclax and a MEK inhibitor did not cause complete cell death (Fig. 2D), we evaluated combined inhibition of PI3K, Bcl-2/Bcl-x_L, and MEK. Activation of the PI3K pathway reduces proapoptotic signaling by promoting an inhibitory phosphorylation of BAD on Ser136 (5) and repressing FOXO3-driven transcription of BIM (37). Thus, inhibition of this pathway is expected to promote proapoptotic signaling by increasing the activity of BAD and the level of BIM. We selected an effective, clinically relevant dose of the PI3K inhibitor GDC-0941 (Fig. 1B; refs. 38–40) and added it to all wells of the navitoclax/G-963 combination matrix on 3 cell lines. In all lines, the overall growth inhibition is enhanced with the addition of GDC-0941, but the patterns of response vary. In the A427 cell line, there is significant enhancement of activity at the higher doses of G-963. This seems to be largely driven by the synergy between of G-963 with the addition of the PI3K, as seen in the G-963/GDC-0941 combination curve on the far right panel of Fig. 4A. In H2122 cells, there is an increase in activity with the

Published OnlineFirst March 8, 2013; DOI: 10.1158/1535-7163.MCT-12-0949

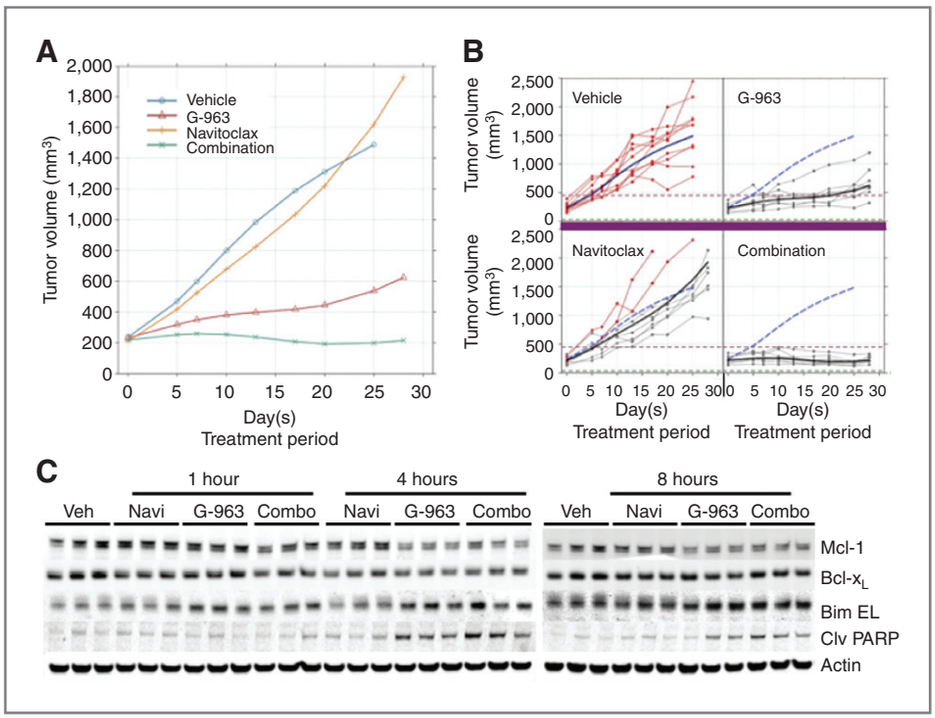

Figure 3. H2122 xenografts exhibit tumor stasis upon treatment with the combination of G-963 and navitoclax. Tumor-bearing mice were dosed orally and daily (QD) for 28 days with 100 mg/kg of navitoclax, 25 mg/kg of G-963 or the combination. A, mean tumor volume from mice treated with vehicle (blue), G-963 (red), navitoclax (yellow), or the combination (green). B, tumor volumes of individual mice with mean tumor volume for the vehicle control group (blue) or each drug-treated group (solid black); dotted blue lines represent the mean tumor volume for the vehicle control for comparison. C, Western blots of H2122 tumor xenografts after a single dose of navitoclax (navi), G-963, or the combination (combo) of both drugs at the indicated times.

addition of GDC-0941 across the entire dose matrix (Fig. 4B), and the effects of G-963 and GDC-0941 seem additive, as seen with the shift of the G-963 dose response with the addition of GDC-941 (Fig. 4B, right). Finally, in the A549 cell line, the enhancement of activity is more pronounced at the lower doses of G-963 (Fig. 4C). These observations highlight the importance of measuring effects across a range of concentrations and ratios to capture the range of response.

Addition of a PI3 kinase inhibitor to the navitoclax/MEK inhibitor combination increases apoptosis

To explore the mechanism of navitoclax/G-963/GDC-0941 triple combination-induced cell death, we measured intrinsic apoptosis by caspase activation and effects on signaling pathway components by Western blotting. The triple combination causes strong activation of caspases 3 and/or 7 as early as 8 hours posttreatment in A427 and H2122 cells (purple bars in Fig. 5A and B), compared with the single- or double-agent treatments in which high levels of caspase activation are not observed until 24 or 48 hours posttreatment. The rapid kinetics of the triple combination might provide an advantage *in vivo* if exposure is limited by the pharmacokinetic properties of the compounds.

Because the differences in response to single-, double-, and triple-agent combinations were most pronounced at 8 hours, we conducted Western blotting of pathway proteins at 2, 8, and 24 hours posttreatment to the capture the relevant time points. MEK inhibition with G-963 alone and in all tested combinations promotes loss of ERK1/2 phosphorylation and decreased p90RSK phosphorylation on S380. There is also an increase in BIM gel mobility, indicative of loss of phosphorylation in all G-963–treated samples; the loss of BIM phosphorylation was confirmed with a phospho-S69–specific antibody. Moreover, induction of p21 (CDKN1A) and p27 (CDKN1B) are observed after 24 hours in all G-963–treated cells, consistent with the observed G_1 arrest (Fig. 5C and D). The activity of GDC-0941 on PI3K was showed by a decrease in phospho-AKT1 (S473) in all treated cells. The addition of navitoclax did not alter the proximal downstream effectors of MEK and PI3K signaling. We next examined BAD phosphorylation following treatment. Surprisingly, navitoclax causes an increase of phosphorylation on BAD at S112 and S136. This may reflect negative feedback loop exerting inhibition on BAD that results from the addition of the "BAD mimetic." However, we do not have a mechanism to account for this observation. Addition of GDC-0941 to navitoclax/G-963 combination reduces phosphorylation of BAD. Consistent with the observations that cells are under stress and undergoing apoptosis following drug treatments, we detect increased γ-H2AX levels and PARP cleavage (Fig. 5C and D).

We evaluated the effect of the triple combination on cell-cycle state and cell death by flow cytometry. There were no significant changes in cell-cycle state or sub-2N content at 8 hours. By 24 hours there was an increase in cells with 2N DNA content (G_1) in G-963 treated cells alone or in combinations, and a small increase in cells with sub-2N content was evident in the navitoclax/G-963 and the triple combination treated cells. By 48 hours there was an increase in cells with sub-2N content in the G-963/navitoclax and G-963/GDC-0941 combinations, 25% in each

Published OnlineFirst March 8, 2013; DOI: 10.1158/1535-7163.MCT-12-0949

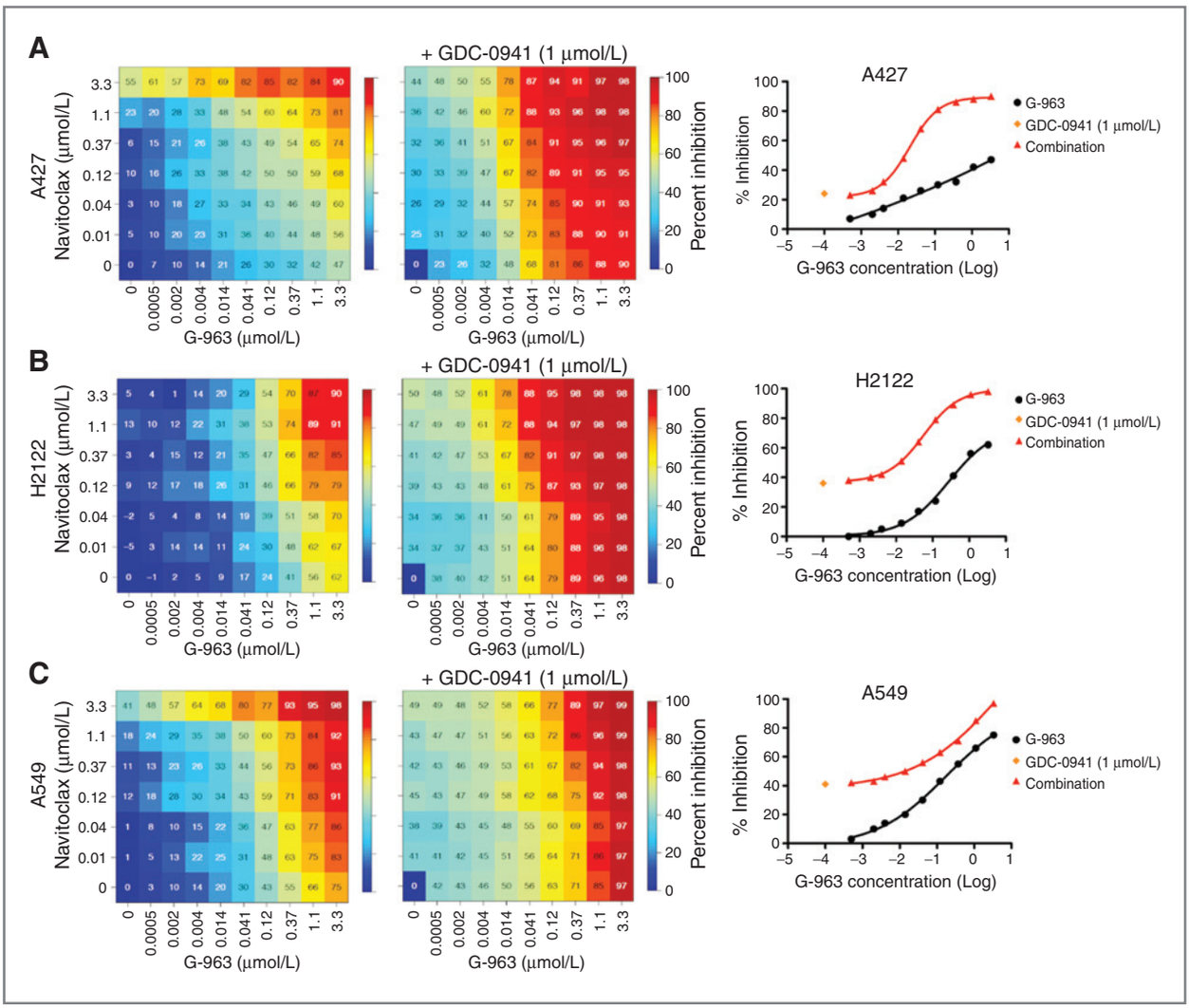

Figure 4. Triple combinations of MEK, PI3 kinase, and Bcl-2/Bcl-x_L inhibitors. Cells were treated in a G-963/navitoclax dose matrix as described and then overlaid with media containing DMSO or 1 μmol/L GDC-0941 as indicated. Growth inhibition across all combinations is represented as a heat map of percent control. For the triple combination, the data are shown as a percent inhibition compared with the untreated control (bottom left). The graphs on the right represent the dose–response curve for G-963 alone and with 1 μmol/L GDC-0941. A, A427 cells; B, H2122 cells; C, A549 cells.

double combination, compared with untreated and single-agent treatment samples which all had less than 5% sub-2N. The percentage of cells with sub-2N content was highest in the triple combination with 41% sub-2N (Fig. 5E).

Discussion

Inhibitors of MEK and PI3K are being tested as single agents and in combination in the clinic. Because efficacy of targeted agents is often limited, we wanted to identify combinations that improve efficacy. MEK inhibitor–mediated cytotoxicity is enhanced by Bcl-2/Bcl-x_L inhibition across a large panel of NSCLC and pancreatic cell lines. MEK inhibition is reported to increase cell death by increasing BIM protein and suppressing inhibitory phosphorylation of BAD. Increased BIM was observed in all cell lines tested, whereas loss of BAD phosphorylation varied, and thus could represent vulnerability in MEK inhibitor–dependent induction of apoptosis. BAD can also be inhibited via activation of the PI3K pathway, making it susceptible to "rewiring" of upstream signaling. Navitoclax can circumvent resistance via rephosphorylation of BAD because it acts a BAD mimetic that is not subject to inhibitory phosphorylation. Stabilization of BIM is likely critical to the mechanism of the combination because it binds to and inhibits the antiapoptotic activity of MCL1, which navitoclax cannot do. Overall, our data are consistent with a model in which the stabilization of BIM observed after MEK inhibition is necessary for inhibition of MCL1, but not sufficient to neutralize all of the antiapoptotic activity of Bcl-2, Bcl-x_L. Navitoclax alone does not induce apoptosis because it can only neutralize

Published OnlineFirst March 8, 2013; DOI: 10.1158/1535-7163.MCT-12-0949

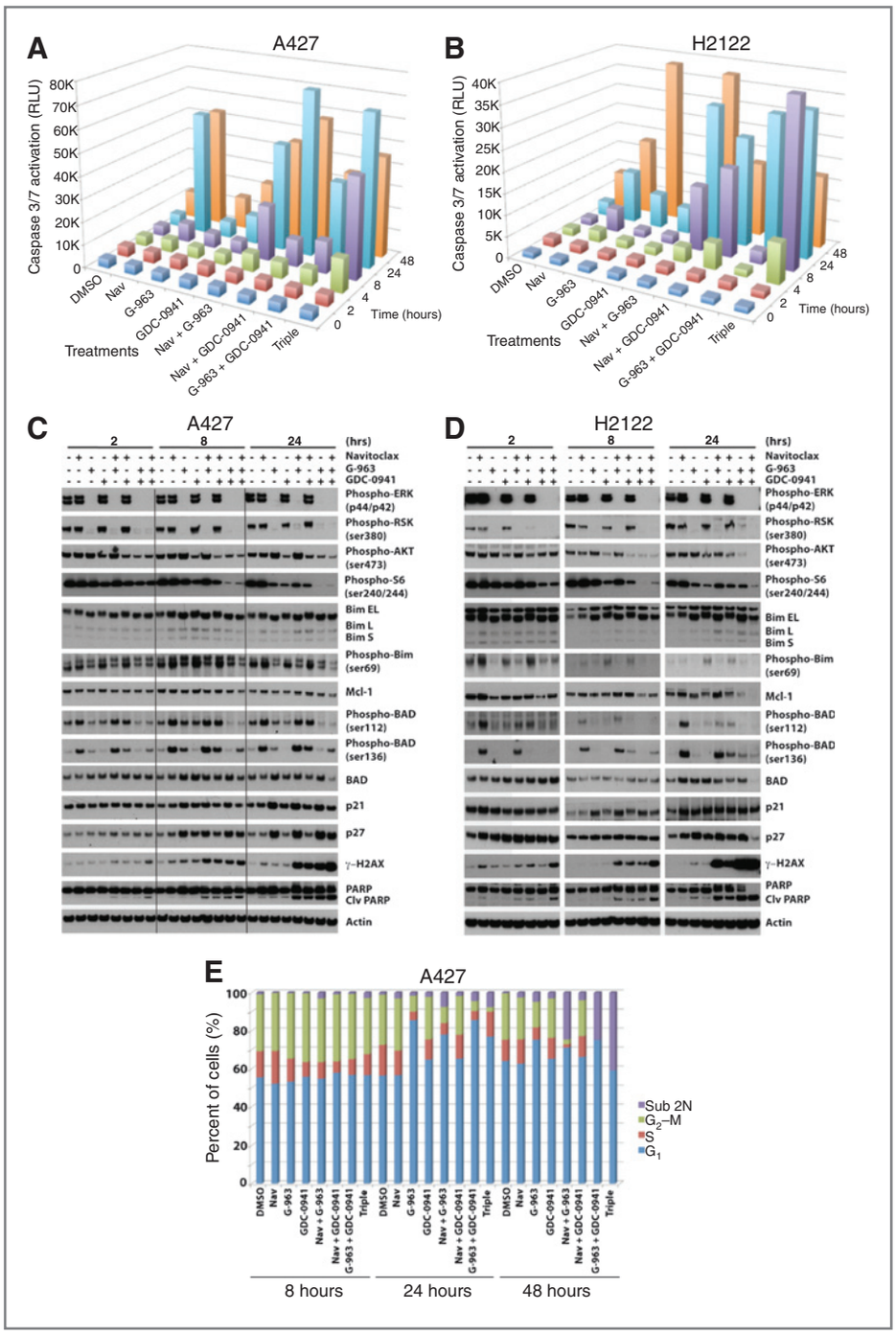

Figure 5. Apoptosis and signaling pathway modulation because of combinations of MEK, PI3 kinase, and Bcl-2/Bcl-x_L inhibitors. A427 (A) and H2122 (B) treated with navitoclax (1 μmol/L), G-963 (2 μmol/L), GDC-0941 (1 μmol/L) alone, or in double or triple combinations. Caspase activation was measured using Caspase-Glo 3/7. Western blots of A427 (C) or H2122 (D) cells treated with the indicated agents for 2, 8, or 24 hours. E, DNA content of A427 cells 8, 24, or 48 hours after treatment.

Bcl-2 and Bcl-x_L, leaving MCL1 to protect the cell. However, in the combination navitoclax neutralizes Bcl-2 and Bcl-x_L, allowing the excess pools of BIM that result from MEK inhibition to neutralize MCL1.

Of the proteins investigated for correlative biomarker studies, only the baseline level of pS112 BAD revealed significant correlation with synergy scores observed for the navitoclax/G-963 combination treatment. These findings suggest that cells with higher levels of phospho-BAD are less likely to benefit from the addition of navitoclax because there is a sufficiently large pool of phosphorylated (inactive) BAD that can be activated upon MEK inhibition to saturate the binding sites on Bcl-x_L and Bcl-2. Although there is preclinical evidence and mechanistic rationale for larger pools of S112 phospho-BAD acting as a negative predictor for synergy, the dynamic

Published OnlineFirst March 8, 2013; DOI: 10.1158/1535-7163.MCT-12-0949

range of baseline phospho-BAD is small and quantitative evaluation of phosphorylated epitope in clinical samples is likely to be challenging. The best correlation of navitoclax/MEK inhibitor synergy was single-agent sensitivity to MEK inhibition. Thus, the same predictive biomarkers relevant for MEK inhibitors, that is activation of the RAS/RAF/MEK pathway, could potentially be used to enrich for response to the combination with navitoclax. An MEK-dependent transcriptional profile could provide the most accurate predictor of pathway activation (41). However, this is challenging to implement as a companion diagnostic. We observed enrichment in activating KRAS mutations the high synergy cell lines and propose that KRAS mutant cancers represent a molecularly defined subset of cancers that may be more likely to respond to a MEK inhibitor navitoclax combination.

The RAS/RAF/MEK/ERK signaling cascade plays an important role in controlling cell proliferation and regulating the cell cycle. ERK activation throughout G_1 and ERK translocation to the nucleus are required for entry to S phase (42–44). Navitoclax does not alter MEK inhibitor-induced G_1 arrest observed at 24 hours, but strongly increases cell death at 48 hours, suggesting that the cells die after entering G_1. The observed cell death is dependent upon caspase activity, but not the extrinsic apoptosis and necrosis kinase, RIP1, consistent with our observation of caspase 3/7 activation and PARP cleavage.

The navitoclax/MEK inhibitor combination effect observed *in vitro* was validated *in vivo* using a human NSCLC H2122 xenograft model. In contrast to each single agent, we observed a combination treatment effect characterized by tumor stasis when navitoclax was coadministered with G-963. We propose that the combination of both agents increased apoptosis in the H2122 NSCLC xenograft model because of antagonism of Bcl-x_L by navitoclax and G-963–induced stabilization of BIM resulting in neutralization of MCL1.

Finally, we show that the triple combination of G-963/GDC-0941/navitoclax has increased activity compared with the double combinations. There is tremendous interest in combining MEK inhibitors with PI3K inhibitors to combat resistance via alternate signaling that suppresses apoptosis. However, the activation of apoptosis can be incomplete even with the combination of these kinase inhibitors. Although studies suggest that Bcl-2/Bcl-x_L inhibitors can enhance efficacy of GDC-0941 in breast cancer models (13, 14), this is the first study to explore the triple combination of navitoclax with both a PI3K and an MEK inhibitor. The addition of the PI3K inhibitor, GDC-0941, to the combination suppresses AKT activation, resulting in increased cytotoxicity as measured by decreased ATP caspase3/7 activation, γ-H2AX induction, increased sub-2N DNA content, and PARP cleavage.

In conclusion, we show the potential benefit of codosing with navitoclax to enhance the activity of a MEK inhibitor, especially in cancers with KRAS mutations. This benefit could be further improved with the addition of a PI3K inhibitor. Although this work was under review, 2 studies independently confirmed the value of combining a MEK inhibitor with navitoclax (45, 46). In light of the broad scope of current clinical evaluation underway with agents targeting the MEK, PI3K and Bcl-2/Bcl-x_L pathways, these findings provide a rationale for clinical testing of previously unrecognized therapeutic combinations.

Disclosure of Potential Conflicts of Interest

No potential conflicts of interest were disclosed.

Authors' Contributions

Conception and design: N. Tan, S. Price, D. Sampath, W. J. Fairbrother, L. D. Belmont
Development of methodology: N. Tan, S. Price
Acquisition of data (provided animals, acquired and managed patients, provided facilities, etc.): N. Tan, M. Wong, M. A. Nannini, R. Hong, L. B. Lee, K. Williams
Analysis and interpretation of data (e.g., statistical analysis, biostatistics, computational analysis): N. Tan, M. Wong, M. A. Nannini, L. B. Lee, K. Williams, P. Yue, D. Sampath, L. D. Belmont
Writing, review, and/or revision of the manuscript: N. Tan, S. Price, D. Sampath, J. Settleman, W. J. Fairbrother, L. D. Belmont
Administrative, technical, or material support (i.e., reporting or organizing data, constructing databases): N. Tan, P. Pascal Savy
Study supervision: N. Tan, M. A. Nannini, D. Sampath

Acknowledgments

The authors thank S. Selvaraj, M. Yu, and R. Neve for providing and authenticating cell lines; M. Belvin and the Abbott Bcl-2 team for helpful input.

The costs of publication of this article were defrayed in part by the payment of page charges. This article must therefore be hereby marked *advertisement* in accordance with 18 U.S.C. Section 1734 solely to indicate this fact.

Received September 26, 2012; revised March 4, 2013; accepted March 4, 2013; published OnlineFirst March 8, 2013.

References

1. Eiring AM, Khorashad JS, Morley K, Deininger MW. Advances in the treatment of chronic myeloid leukemia. BMC Med 2011; 9:99.
2. Wong K-K, Engelman JA, Cantley LC. Targeting the PI3K signaling pathway in cancer. Curr Opin Genet Dev 2010;20:87–90.
3. Hoeflich KP, Merchant M, Orr C, Chan J, Otter Den D, Berry L, et al. Intermittent administration of MEK inhibitor GDC-0973 plus PI3K inhibitor GDC-0941 triggers robust apoptosis and tumor growth inhibition. Cancer Res 2012;72:210–9.
4. Kinross KM, Brown DV, Kleinschmidt M, Jackson S, Christensen J, Cullinane C, et al. *In vivo* activity of combined PI3K/mTOR and MEK inhibition in a KrasG12D;pten deletion mouse model of ovarian cancer. Mol Cancer Ther 2011;10:1440–9.
5. She Q-B, Solit DB, Ye Q, O'Reilly KE, Lobo J, Rosen N. The BAD protein integrates survival signaling by EGFR/MAPK and PI3K/Akt kinase pathways in PTEN-deficient tumor cells. Cancer Cell 2005;8: 287–97.
6. Aksamitiene E, Kiyatkin A, Kholodenko BN. Cross-talk between mitogenic Ras/MAPK and survival PI3K/Akt pathways: a fine balance. Biochem Soc Trans 2012;40:139–46.
7. De Luca A, Maiello MR, D'Alessio A, Pergameno M, Normanno N. The RAS/RAF/MEK/ERK and the PI3K/AKT signalling pathways: role in

Published OnlineFirst March 8, 2013; DOI: 10.1158/1535-7163.MCT-12-0949

cancer pathogenesis and implications for therapeutic approaches. Expert Opin Ther Targets 2012;16:S17–27.
8. Corcoran RB, Settleman J, Engelman JA. Potential therapeutic strategies to overcome acquired resistance to BRAF or MEK inhibitors in BRAF mutant cancers. Oncotarget 2011;1–11.
9. Poulikakos PI, Solit DB. Resistance to MEK inhibitors: should we co-target upstream? Sci Signal 2011;4:pe16.
10. Greger JG, Eastman SD, Zhang V, Bleam MR, Hughes AM, Smitheman KN, et al. Combinations of BRAF, MEK, and PI3K/mTOR inhibitors overcome acquired resistance to the BRAF inhibitor GSK2118436 dabrafenib, mediated by NRAS or MEK mutations. Mol Cancer Ther 2012;11:909–20.
11. Shimizu T, Tolcher AW, Papadopoulos KP, Beeram M, Rasco D, Smith LS, et al. The clinical effect of the dual-targeting strategy involving PI3K/AKT/mTOR and RAS/MEK/ERK pathways in patients with advanced cancer. Clin Cancer Res 2012;18:2316–25.
12. Cragg MS, Jansen ES, Cook M, Harris C, Strasser A, Scott CL. Treatment of B-RAF mutant human tumor cells with a MEK inhibitor requires BIM and is enhanced by a BH3 mimetic.J Clin Invest 2008; 118:3651–9.
13. Zheng L, Yang W, Zhang C, Ding W-J, Zhu H, Lin N-M, et al. GDC-0941 sensitizes breast cancer to ABT-737 *in vitro* and *in vivo* through promoting the degradation of Mcl-1. Cancer Lett 2011;309: 27–36.
14. Muranen T, Selfors LM, Worster DT, Iwanicki MP, Song L, Morales FC, et al. Inhibition of PI3K/mTOR leads to adaptive resistance in matrix-attached cancer cells. Cancer Cell 2012;21:227–39.
15. Dehan E, Bassermann F, Guardavaccaro D, Vasiliver-Shamis G, Cohen M, Lowes KN, et al. βTrCP- and Rsk1/2-mediated degradation of BIMEL inhibits apoptosis. Mol Cell 2009;33:109–16.
16. Yang J-Y, Zong CS, Xia W, Yamaguchi H, Ding Q, Xie X, et al. ERK promotes tumorigenesis by inhibiting FOXO3a via MDM2-mediated degradation. Nat Cell Biol 2008;10:138–48.
17. Domina AM, Vrana JA, Gregory MA, Hann SR, Craig RW. MCL1 is phosphorylated in the PEST region and stabilized upon ERK activation in viable cells, and at additional sites with cytotoxic okadaic acid or taxol. Oncogene 2004;23:5301–15.
18. Brunelle JK, Letai A. Control of mitochondrial apoptosis by the Bcl-2 family. J Cell Sci 2009;122:437–41.
19. Tse C, Shoemaker AR, Adickes J, Anderson MG, Chen J, Jin S, et al. ABT-263: a potent and orally bioavailable Bcl-2 family inhibitor. Cancer Res 2008;68:3421–8.
20. Ackler S, Mitten MJ, Foster K, Oleksijew A, Refici M, Tahir SK, et al. The Bcl-2 inhibitor ABT-263 enhances the response of multiple chemotherapeutic regimens in hematologic tumors *in vivo*. Cancer Chemother Pharmacol 2010;66:869–80.
21. Wong M, Tan N, Zha J, Peale FV, Yue P, Fairbrother WJ, et al. Navitoclax (ABT-263) reduces Bcl-xL-mediated chemoresistance in ovarian cancer models. Mol Cancer Ther 2012;11:1026–35.
22. Shi J, Zhou Y, Huang HC, Mitchison TJ. Navitoclax (ABT-263) accelerates apoptosis during drug-induced mitotic arrest by antagonizing Bcl-xL. Cancer Res 2011;71:4518–26.
23. Chen J, Jin S, Abraham V, Huang X, Liu B, Mitten MJ, et al. The Bcl-2/Bcl-XL/Bcl-w inhibitor, navitoclax, enhances the activity of chemotherapeutic agents *in vitro* and *in vivo*. Mol Cancer Ther 2011;10: 2340–9.
24. Tan N, Malek M, Zha J, Yue P, Kassees R, Berry L, et al. Navitoclax enhances the efficacy of taxanes in non-small cell lung cancer models. Clin Cancer Res 2011;17:1394–404.
25. Konopleva M, Milella M, Ruvolo P, Watts JC, Ricciardi MR, Korchin B, et al. MEK inhibition enhances ABT-737-induced leukemia cell apoptosis via prevention of ERK-activated MCL1induction and modulation of MCL-1/BIM complex. Leukemia 2012;26:778–87.
26. Lehár J, Stockwell BR, Giaever G, Nislow C. Combination chemical genetics. Nat Chem Biol 2008;4:674–81.
27. JC P, DM B. Mixed-effects models in S and S-PLUS. New York: Springer-Verlag; 2000.
28. Wilson WH, O'Connor OA, Czuczman MS, LaCasce AS, Gerecitano JF, Leonard JP, et al. Navitoclax, a targeted high-affinity inhibitor of BCL-2, in lymphoid malignancies: a phase 1 dose-escalation study of safety, pharmacokinetics, pharmacodynamics, and antitumour activity. Lancet Oncol 2010;11:1149–59.
29. Roberts AW, Seymour JF, Brown JR, Wierda WG, Kipps TJ, Khaw SL, et al. Substantial susceptibility of chronic lymphocytic leukemia to BCL2 inhibition: results of a phase I study of navitoclax in patients with relapsed or refractory disease. J Clin Oncol 2012;30:488–96.
30. Gandhi L, Camidge DR, Ribeiro de Oliveira M, Bonomi P, Gandara D, Khaira D, et al. Phase I study of navitoclax (ABT-263), a novel Bcl-2 family inhibitor, in patients with small-cell lung cancer and other solid tumors. J Clin Oncol 2011;29:909–16.
31. Rudin CM, Hann CL, Garon EB, Ribeiro de Oliveira M, Bonomi PD, Camidge DR, et al. Phase II study of single-agent navitoclax (ABT-263) and biomarker correlates in patients with relapsed small cell lung cancer. Clin Cancer Res 2012;18:3163–9.
32. Jing J, Greshock J, Holbrook JD, Gilmartin A, Zhang X, McNeil E, et al. Comprehensive predictive biomarker analysis for MEK inhibitor GSK1120212. Mol Cancer Ther 2012;11:720–9.
33. Garon EB, Finn RS, Hosmer W, Dering J, Ginther C, Adhami S, et al. Identification of common predictive markers of *in vitro* response to the MEK inhibitor selumetinib (AZD6244; ARRY-142886) in human breast cancer and non-small cell lung cancer cell lines. Mol Cancer Ther 2010;9:1985–94.
34. Tentler JJ, Nallapareddy S, Tan AC, Spreafico A, Pitts TM, Morelli MP, et al. Identification of predictive markers of response to the MEK1/2 inhibitor selumetinib (AZD6244) in K-ras-mutated colorectal cancer. Mol Cancer Ther 2010;9:3351–62.
35. Dry JR, Pavey S, Pratilas CA, Harbron C, Runswick S, Hodgson D, et al. Transcriptional pathway signatures predict MEK addiction and response to selumetinib (AZD6244). Cancer Res 2010;70:2264–73.
36. Degterev A, Hitomi J, Germscheid M, Ch'en IL, Korkina O, Teng X, et al. Identification of RIP1 kinase as a specific cellular target of necrostatins. Nat Chem Biol 2008;4:313–21.
37. Tzivion G, Dobson M, Ramakrishnan G. FoxO transcription factors: regulation by AKT and 14-3-3 proteins. Biochim Biophys Acta 2011;1813:1938–45.
38. Folkes AJ, Ahmadi K, Alderton WK, Alix S, Baker SJ, Box G, et al. The identification of 2-(1 H-Indazol-4-yl)-6-(4-methanesulfonyl-piperazin-1-ylmethyl)-4-morpholin-4-yl-thieno[3,2- d]pyrimidine (GDC-0941) as a potent, selective, orally bioavailable inhibitor of class I PI3 kinase for the treatment of cancer †. J Med Chem 2008;51:5522–32.
39. Salphati L, Wong H, Belvin M, Bradford D, Edgar KA, Prior WW, et al. Pharmacokinetic-pharmacodynamic modeling of tumor growth inhibition and biomarker modulation by the novel phosphatidylinositol 3-kinase inhibitor GDC-0941. Drug Metab Dispos 2010;38:1436–42.
40. Salphati L, Pang J, Plise EG, Chou B, Halladay JS, Olivero AG, et al. Preclinical pharmacokinetics of the novel PI3K inhibitor GDC-0941 and prediction of its pharmacokinetics and efficacy in human. Xenobiotica 2011;41:1088–99.
41. Pratilas CA, Taylor BS, Ye Q, Viale A, Sander C, Solit DB, et al. (V600E) BRAF is associated with disabled feedback inhibition of RAF-MEK signaling and elevated transcriptional output of the pathway. Proc Natl Acad Sci USA 2009;106:4519–24.
42. Yamamoto T, Ebisuya M, Ashida F, Okamoto K, Yonehara S, Nishida E. Continuous ERK activation downregulates antiproliferative genes throughout G1 phase to allow cell-cycle progression. Curr Biol 2006;16:1171–82.
43. Jones SM, Kazlauskas A. Growth-factor-dependent mitogenesis requires two distinct phases of signalling. Nat Cell Biol 2001;3:165–72.
44. Brunet A, Roux D, Lenormand P, Dowd S, Keyse S, Pouysségur J. Nuclear translocation of p42/p44 mitogen-activated protein kinase is required for growth factor-induced gene expression and cell cycle entry. EMBO J 1999;18:664–74.
45. Corcoran RB, Cheng KA, Hata AN, Faber AC, Ebi H, Coffee EM, et al. Synthetic lethal interaction of combined BCL-XL and MEK inhibition promotes tumor regressions in KRAS mutant cancer models. Cancer Cell 2013;23:121–8.
46. Sale M, Cook S. The BH3-mimetic ABT-263 synergizes with the MEK1/2 inhibitor selumetinib/AZD6244 to promote BIM-dependent tumour cell death and inhibit acquired resistance. Biochem J 2013;450: 285–94.

Published OnlineFirst March 8, 2013; DOI: 10.1158/1535-7163.MCT-12-0949

Molecular Cancer Therapeutics

Bcl-2/Bcl-x_L Inhibition Increases the Efficacy of MEK Inhibition Alone and in Combination with PI3 Kinase Inhibition in Lung and Pancreatic Tumor Models

Nguyen Tan, Maureen Wong, Michelle A. Nannini, et al.

Mol Cancer Ther 2013;12:853-864. Published OnlineFirst March 8, 2013.